

On the Nature of Charge Transport in Quantum-Cascade Lasers

Rita Claudia Iotti^{1,2} and Fausto Rossi¹

¹*Istituto Nazionale per la Fisica della Materia (INFN) and Dipartimento di Fisica, Politecnico di Torino, Corso Duca degli Abruzzi 24, 10129 Torino, Italy*

²*Scuola Normale Superiore, Piazza dei Cavalieri 7, 56126 Pisa, Italy*

(October 24, 2018)

The first *global quantum simulation* of semiconductor-based quantum-cascade lasers is presented. Our three-dimensional approach allows to study in a purely microscopic way the current-voltage characteristics of state-of-the-art unipolar nanostructures, and therefore to answer the long-standing controversial question: *is charge transport in quantum-cascade lasers mainly coherent or incoherent?* Our analysis shows that: (i) Quantum corrections to the semiclassical scenario are minor; (ii) Inclusion of carrier-phonon and carrier-carrier scattering gives excellent agreement with experimental results.

72.10.-d, 72.20.Ht, 73.63.-b, 78.67.-n

Since the seminal paper of Esaki and Tsu [1], semiconductor-based nanometric heterostructures have been the subject of an impressive theoretical and experimental activity, due to their high potential impact in both fundamental and applied research [2,3]. One of the main fields of research focuses on exploiting “band-gap engineering”, namely the splitting of the bulk conduction band into several subbands, to generate and detect electromagnetic radiation in the infrared spectral region, as originally envisioned by Kazarinov and Suris [4].

Unipolar coherent-light sources like quantum-cascade lasers (QCLs) [5] are complex devices, whose core is a multi-quantum-well (MQW) structure made up of repeated stages of active regions sandwiched between electron-injecting and collecting regions. When a proper bias is applied, an “electron cascade” along the subsequent quantized-level energy staircase takes place. QCLs are usually modelled in terms of n -level systems [6]. As pointed out in [7], such a macroscopic modeling can only operate as an *a posteriori* fitting procedure. In contrast, for a detailed understanding of the basic physical processes involved, a fully three-dimensional (3D) description is needed. More specifically, two main issues need to be addressed: (i) the nature of the hot-carrier relaxation within the device active region; (ii) the nature —coherent versus incoherent— of the physical mechanisms governing charge transport through injector/active-region/collector interfaces.

Point (i) has been recently addressed in [7], where the usual macroscopic treatment of the device active region has been compared to a fully kinetic description, based on a Monte Carlo (MC) solution [8] of the following set of equations:

$$\frac{d}{dt}f_{\mathbf{k}\nu} = [g_{\mathbf{k}\nu} - \Gamma_{\mathbf{k}\nu}f_{\mathbf{k}\nu}]_{i/l} + \sum_{\mathbf{k}'\nu'} [P_{\mathbf{k}\nu, \mathbf{k}'\nu'} f_{\mathbf{k}'\nu'} - P_{\mathbf{k}'\nu', \mathbf{k}\nu} f_{\mathbf{k}\nu}] \quad (1)$$

Here, the first two terms describe —still on a partially

phenomenological level— injection/loss (i/l) of carriers with parallel or in-plane wavevector \mathbf{k} in subband ν , while the last ones describe intra- as well as inter-subband in- and out-scattering processes ($\mathbf{k}\nu \rightarrow \mathbf{k}'\nu'$). As reported in [7], the quantum-cascade within the active region is mainly governed by LO-phonon emission. However, such a microscopic analysis, being limited to the device active region only, does not allow to answer point (ii); This issue is intimately related to the long-standing controversial question [9]: *is charge transport in quantum-cascade lasers mainly coherent or incoherent?*

To provide a definite answer to this fundamental question, we present the first *global quantum simulation* —injector plus active region plus collector— of semiconductor-based QCL structures. To this end, two basic steps are needed: First, the partially phenomenologic model in (1) has to be replaced by a fully microscopic description of the whole MQW core structure; Second, the semiclassical or Boltzmann-like treatment will be replaced by a fully quantum-mechanical one. These are not trivial tasks.

The first step requires a proper simulation scheme to “close the circuit” without resorting to phenomenological i/l parameters. To this aim, given the set of 3D single-particle electron states $\{\mathbf{k}\nu\}$ corresponding to a single QCL stage, we consider the ideal MQW structure obtained as infinite repetition of this QCL periodicity region (see Fig. 1). Within such extended scheme, the time evolution of the carrier distribution function $f_{\mathbf{k}\alpha}$ is governed by the following Boltzmann-like equation:

$$\frac{d}{dt}f_{\mathbf{k}\alpha} = \sum_{\mathbf{k}'\alpha'} [P_{\mathbf{k}\alpha, \mathbf{k}'\alpha'} f_{\mathbf{k}'\alpha'} - P_{\mathbf{k}'\alpha', \mathbf{k}\alpha} f_{\mathbf{k}\alpha}] \quad (2)$$

Here, $\alpha \equiv (\lambda, \nu)$ denotes the generic electron state in our MQW structure, i.e., the ν -th state of the λ -th stage. To “close the circuit”, we impose periodic boundary conditions limiting the inter-stage ($\lambda' \neq \lambda$) scattering to just nearest-neighbor coupling ($\lambda' = \lambda \pm 1$). In view of the translational symmetry, we are allowed to simulate

carrier transport over the central —i.e., $\lambda = 0$ — stage only [10].

We have applied the above —still semiclassical— global-simulation scheme to state-of-the-art QCL structures. As prototypical device, we have considered the GaAs/(Al,Ga)As-based diagonal-configuration QCL in [11], schematically depicted in Fig. 1, in which our simulation strategy is also sketched. Here, the energy levels and probability densities of various electron states within the simulated stage ($\lambda = 0$) are plotted: They correspond to the device active region ($\nu = 1, 2, 3$ according to the standard notation) as well as to the collector region ($\nu = A, B, C, D, E$). In order to properly model phase-breaking hopping processes, in addition to carrier-optical phonon scattering, all various intra- as well as intersubband carrier-carrier interaction mechanisms have been considered [12].

As a starting point, we have investigated the relative weight of the carrier-carrier and carrier-phonon competing energy-relaxation channels. The time evolution of the carrier population in the various subbands as well as of the total current density are depicted in Fig. 2. Parts (a) and (b) report the population dynamics without and with two-body carrier-carrier scattering, respectively. In our “charge-conserving” scheme, we start the simulation assuming the total number of carriers to be equally distributed among the different subbands; then the electron distribution functions evolve according to Eq. (2) and a steady-state condition is eventually reached, leading to the desired $3 \rightarrow 2$ population inversion. As we can see, the inclusion of intercarrier scattering has significant effects: It strongly increases inter-subband carrier redistribution, thus reducing the electron accumulation in the lowest energy level A and optimizing the coupling between active region and injector/collector (the populations of subbands 3 and B get equal). This effect comes out to be crucial in determining the electron flux through the MQW structure. Figure 2(c) shows the simulated current-voltage characteristics of our QCL device, obtained with and without carrier-carrier interaction. At the threshold operating parameters estimated in [11] [marked by an arrow in Fig. 2(c)] the current density in the presence of both electron-phonon and electron-electron scattering mechanisms is about 4 kA/cm². This value is in relatively good agreement with experiments [13].

The results plotted in fig. 2 clearly demonstrate that within a purely semiclassical picture the electron-phonon interaction alone is not able to efficiently couple the injector subbands to the active region ones: While carrier-phonon relaxation well describes the electronic quantum cascade within the bare active region [7], carrier-carrier scattering plays an essential role in determining charge transport through the full core region. This can be ascribed to two typical features of carrier-carrier interaction —compared to the case of carrier-phonon—: (i) this is a

long-range two-body interaction mechanism, which also couples non-overlapping single-particle states [see Fig. 1]; (ii) the corresponding scattering process at relatively low carrier density is quasielastic, thus coupling nearly resonant energy levels, like states 3 and B.

So far, no quantum mechanical effects, like coherent resonant tunneling between adjacent states, have been considered. In order to see how such coherent phenomena can change the scenario presented so far, we have extended our semiclassical simulation scheme in terms of a density-matrix formalism [14]. In the proposed quantum-transport approach the basic ingredient is the single-particle density matrix $\rho_{ij} = \langle a_i^\dagger a_j \rangle$, where a_i^\dagger (a_i) denote creation (destruction) operators for a carrier in state $i \equiv \mathbf{k}\alpha$ [15]. Its time evolution is given by:

$$\frac{d}{dt}\rho_{ij} = -i\omega_{ij}\rho_{ij} + \sum_{i'j'} [(\Gamma_{ij,i'j'}^{\text{in}}\rho_{i'j'} - \Gamma_{ij,i'j'}^{\text{out}}\rho_{i'j'}) + \text{c.c.}] , \quad (3)$$

where $\hbar\omega_{ij} = \epsilon_i - \epsilon_j$ is the energy difference between states i and j . Here, the first term describes the coherent evolution of the noninteracting carrier system while the second contribution describes energy relaxation as well as dephasing, in terms of the generalized in- and out-scattering superoperators Γ [16]. Equation (3) is the desired quantum-mechanical generalization of the Boltzmann transport equation in (2).

Analogous to our semiclassical simulation scheme, for the new quantum-transport formalism we can adopt the same periodic conditions to “close the circuit”. Moreover, since for the QCL design considered in-plane and along- z carrier dynamics are strongly decoupled [17], it is possible to adopt a factorization of the density matrix according to $\rho_{ii'} = \rho_{\mathbf{k}\nu,\mathbf{k}'\nu'} = \rho_{\nu\nu'} f_{\mathbf{k}}^{\parallel} \delta_{\mathbf{k},\mathbf{k}'}$, where f^{\parallel} denotes the parallel or in-plane carrier distribution. This allows us to obtain an effective equation of motion for $\rho_{\nu\nu'}$: the latter, which has again the structure of Eq. (3), involves effective scattering matrices, given by an in-plane average of the quantities $\Gamma^{\text{in/out}}$ in (3).

Comparing the results obtained with the proposed quantum-transport approach to those of the semiclassical global simulation scheme, we find negligible quantum corrections (of a few percents) to the stationary current density. In the absence of carrier-carrier scattering, we get, e.g., a 2% quantum correction to the result at threshold reported in Fig. 2. This is due to the extremely small value of non diagonal density-matrix elements $\rho_{\nu \neq \nu'}$ (compared to the diagonal ones). The physical interpretation of such a behaviour proceeds as follows: Non-diagonal elements in $\Gamma^{\text{in/out}}$ tend to maintain a non-diagonal density matrix also in stationary conditions. On the other hand, diagonal energy-relaxation and dephasing processes tend to suppress non-diagonal terms on the sub-picosecond time-scale. Since the average de-

vice transit time is of the order of several picoseconds, the degree of coherence, i.e., the weight of non-diagonal density-matrix elements, in stationary conditions is very small. This does not mean that coherent phenomena, like resonant-tunneling processes, are not present. Figure 3 presents the first simulation of the ultrafast dynamics of a properly tailored electron wavepacket, within the MQW core region of the QCL sketched in Fig. 1. The aim is to focus on the injector—active-region tunneling mechanisms. For this reason, the system has been prepared at time $t = 0$ to reproduce a charge-density distribution fully localized in the $\lambda = 0$ injector and compatible with resonant tunneling into the next-stage active region (see (0,B)-(+1,3) alignment in Fig. 1). As clearly shown, the transient dynamics is characterized by a strong interplay between phase-coherence and relaxation (on a picosecond time-scale); Only at much longer times it will eventually reach the stationary transport solution, in which incoherent sequential tunneling is the dominant interwell mechanism [18].

In summary, we are in the position to answer the long-standing controversial question on the nature —coherent versus incoherent— of charge transport in QCLs previously mentioned: For the typical structures considered, energy-relaxation and dephasing processes are so strong to destroy any phase-coherence effect on a sub-picosecond time-scale; as a result, the usual semiclassical or incoherent description of stationary charge transport is found to be in excellent agreement with experiments.

We are grateful to F. Beltram, C. Sirtori and A. Tredicucci for fruitful conversations and discussions. This work has been partially supported by the European Commission through the Brite Euram UNISEL project and the FET WANTED project.

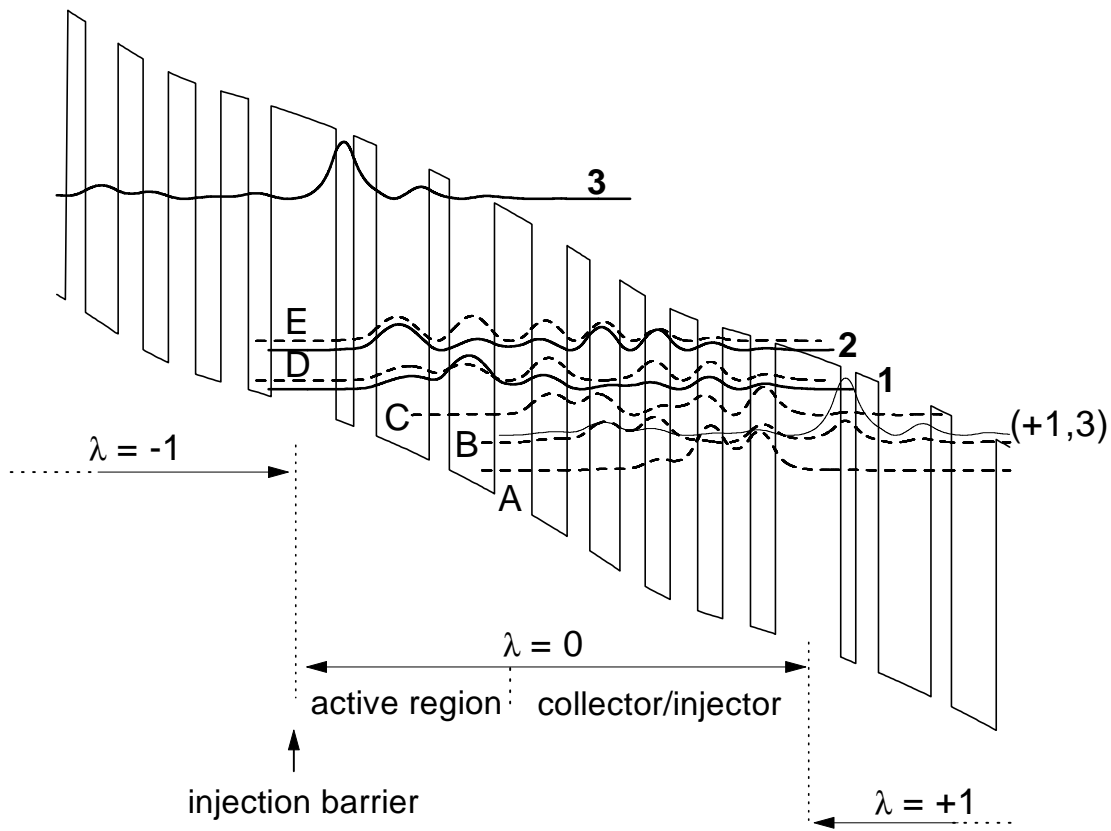
[1] L. Esaki and R. Tsu, *IBM J. Res. Develop.*, **14**, 61 (1970).
[2] See, e.g., J. Shah, *Ultrafast Spectroscopy of Semiconductors and Semiconductor Nanostructures* (Springer, Berlin, 1996); *Theory of Transport Properties of Semiconductor Nanostructures*, edited by E. Schöll (Chapman & Hall, London, 1998).
[3] See, e.g., *Physics of Quantum Electron Devices*, edited by F. Capasso (Springer, Berlin, 1990).
[4] R. F. Kazarinov and R. A. Suris, *Fiz. Tekh. Poluprov.* **5**, 797 (1971); *Sov. Phys. Semicond.* **5**, 707 (1971).
[5] J. Faist *et al.*, *Science* **264**, 553 (1994); G. Scamarcio *et al.*, *Science* **276**, 773 (1997); C. Gmachl *et al.*, *Science* **286**, 749 (1999).
[6] The theoretical description of QCLs is often grounded on purely macroscopic models, which neglect the existence of transverse or “in-plane” degrees of freedom.

[7] R. C. Iotti and F. Rossi, *Appl. Phys. Lett.* **76**, 2265 (2000), and references therein.
[8] See, e.g., C. Jacoboni and P. Lugli, *The Monte Carlo Method for Semiconductor Device Simulations* (Springer, Vienna, 1989).
[9] C. Sirtori *et al.* *IEEE J. Quantum Electron.* **34**, 1722 (1998).
[10] Every time a carrier in state ν undergoes an inter-stage scattering process (i.e., $0, \nu \rightarrow \pm 1, \nu'$), it is properly reinjected into the central region ($0, \nu \rightarrow 0, \nu'$) and the corresponding electron charge $\pm e$ will contribute to the current through the device. This allows for a purely microscopic evaluation of the current-voltage characteristics.
[11] C. Sirtori *et al.*, *Appl. Phys. Lett.* **73**, 3486 (1998).
[12] Other scattering mechanisms not included in the simulation, e.g., carrier—acoustic-phonon coupling, are expected to play a minor role [8].
[13] The apparent discrepancy between the theoretical and the experimental ($\simeq 7 \text{ kA/cm}^2$) results is due, we believe, to the different estimate of the potential drop per period required to line up the ground state A of the injector with level 3 of the active region. Indeed, our Schrödinger-Poisson calculation predicts a good alignment at a higher bias, which agrees much better with the measured one [11].
[14] T. Kuhn, in *Theory of Transport Properties of Semiconductor Nanostructures*, edited by E. Schöll (Chapman & Hall, London, 1998), p. 173.
[15] This is defined as the average value of two creation and destruction operators: its diagonal elements correspond to the usual distribution functions $f_{\mathbf{k}\alpha}$ of the semiclassical Boltzmann theory while the off-diagonal terms ($i \neq j$) describe the degree of quantum-mechanical phase coherence between states i and j .
[16] The in- and out-scattering matrices Γ in (3) describe the effect on the time evolution of the density-matrix element ρ_{ij} due to the generic element $\rho_{i'j'}$. Their diagonal parts, i.e., $ii' = jj'$, correspond to the semiclassical scattering rates $P_{ii'} \equiv P_{\mathbf{k}\alpha, \mathbf{k}'\alpha'}$ in Eq. (2) [14].
[17] R.C. Iotti and F. Rossi, *Appl. Phys. Lett.* **78**, 2902 (2001).
[18] These results suggest that ultrafast optical experiments, like pump-and-probe or four-wave-mixing measurements, should provide a clear fingerprint of such a coherent vs. energy-relaxation carrier dynamics. This is confirmed by recent ultrafast experiments by Eickemeyer *et al.* [F. Eickemeyer *et al.*, to appear in the Proceedings of the 12th International Conference on Nonequilibrium Carrier Dynamics in Semiconductors (HCIS12, Santa Fe, 2001)].

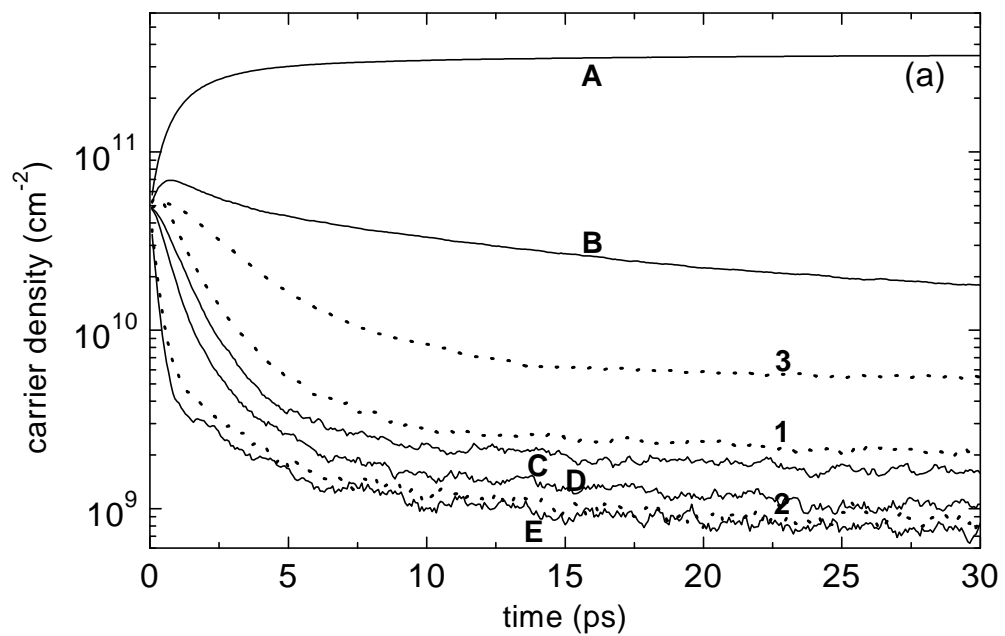
FIG. 1. Schematic representation of the conduction-band profile along the growth direction for the diagonal-configuration QCL structure of Ref. [11]. The MQW is biased by an electric field of 48 kV/cm. The levels $\nu = 1, 2, 3$ and $\nu = \text{A, B, C, D, E}$ in the active and collector regions (full and dashed lines, respectively) of the simulated stage ($\lambda = 0$) are also plotted together with the corresponding probability densities. The replica of level 3 in the following stage $\lambda = +1$ is shown for clarity.

FIG. 2. Time evolution of simulated carrier densities in the various subbands of the MQW structure of Fig. 1 (full lines: $\nu = A, B, C, D, E$; dotted lines: $\nu = 1, 2, 3$), without (a) and with (b) intercarrier scattering. (c): simulated applied-field vs current-density characteristics of the whole structure at 77 K, in presence (discs) and absence (filled squares) of carrier-carrier interaction. Threshold applied field (48 kV/cm) is marked by an arrow. Dashed lines are a guide to the eye.

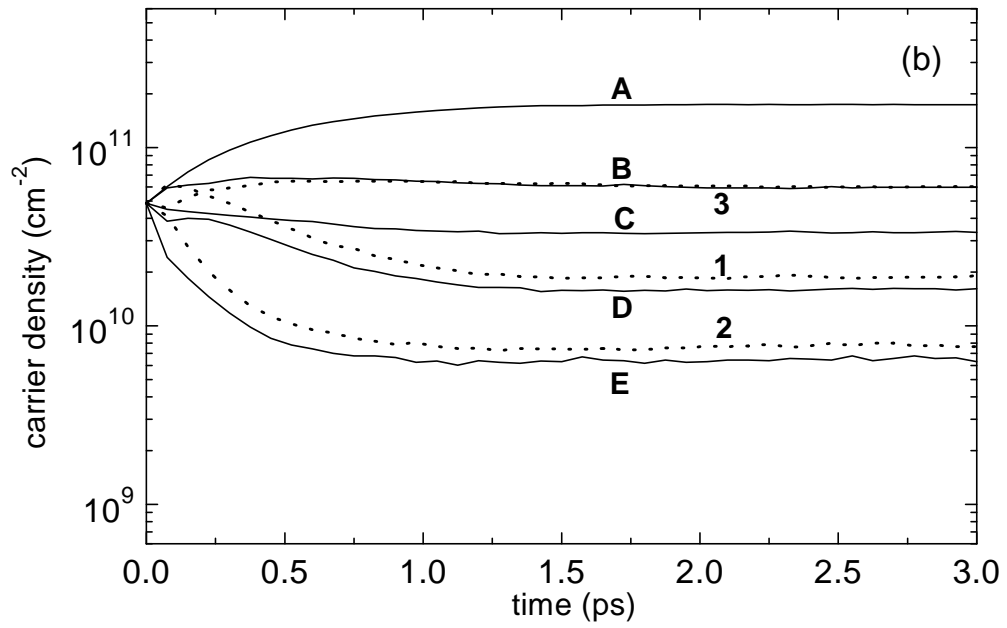
FIG. 3. Time evolution of the charge density for an electron wavepacket properly tailored to study the carrier tunneling dynamics across the injection barrier, for the QCL design of Fig. 1. At $t = 0$ ps (lower panel (c)) the wavepacket is fully localized in the injector. Shaded regions correspond to (Al,Ga)As barriers in the heterostructure design. The transient dynamics (middle panel (b)) is characterized by a strong interplay between phase-coherence and relaxation processes. At much longer times (upper panel (a)) the system will eventually evolve into the stationary transport solution.



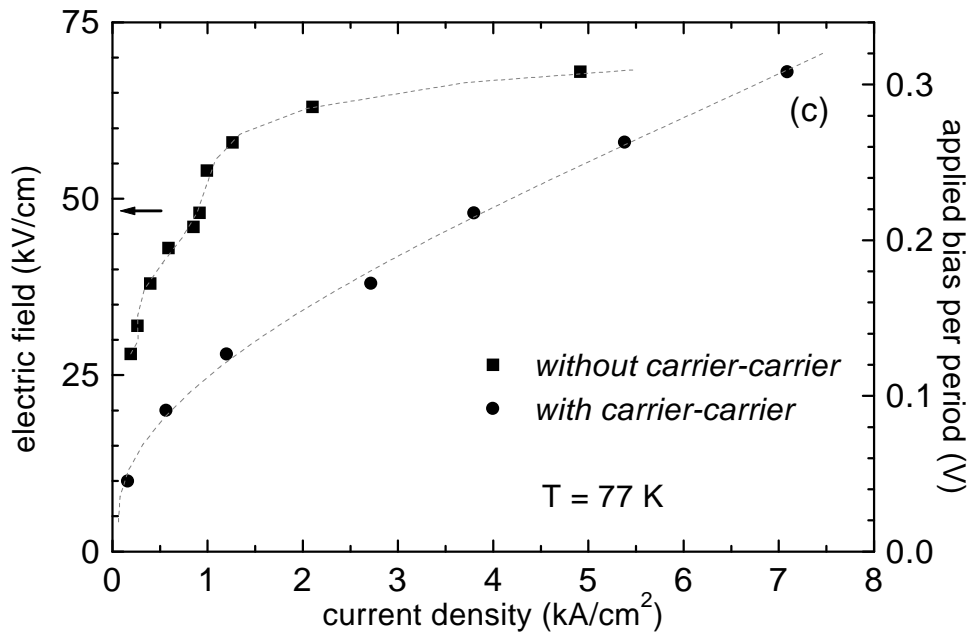
R. C. Iotti and F. Rossi, Figure 1



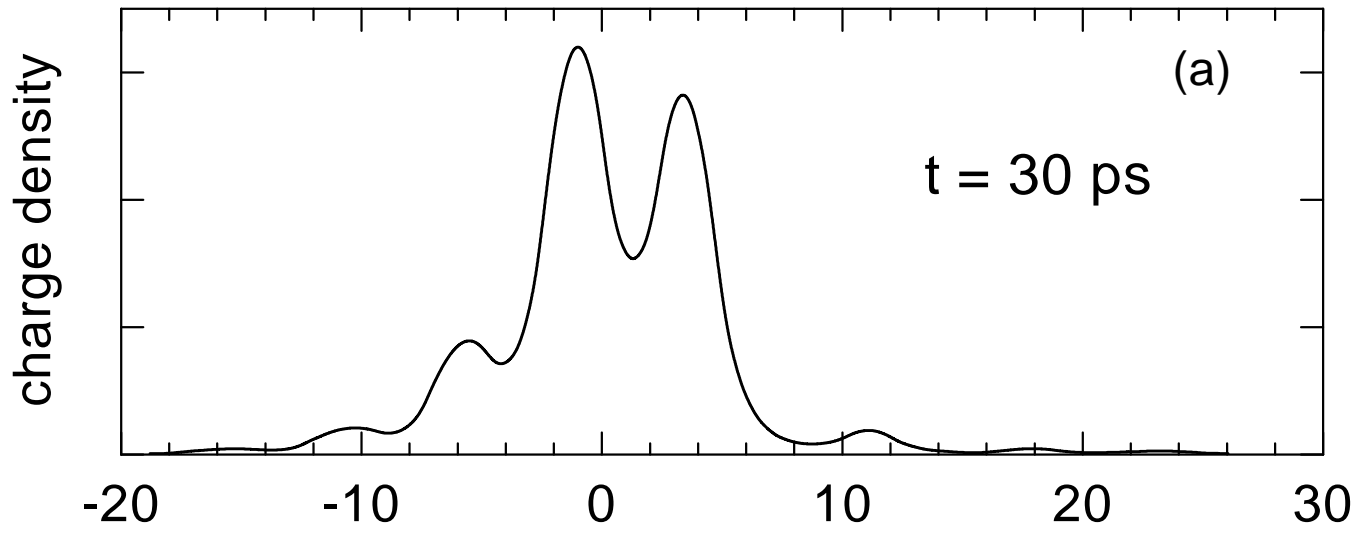
R. C. Iotti and F. Rossi, Figure 2(a)



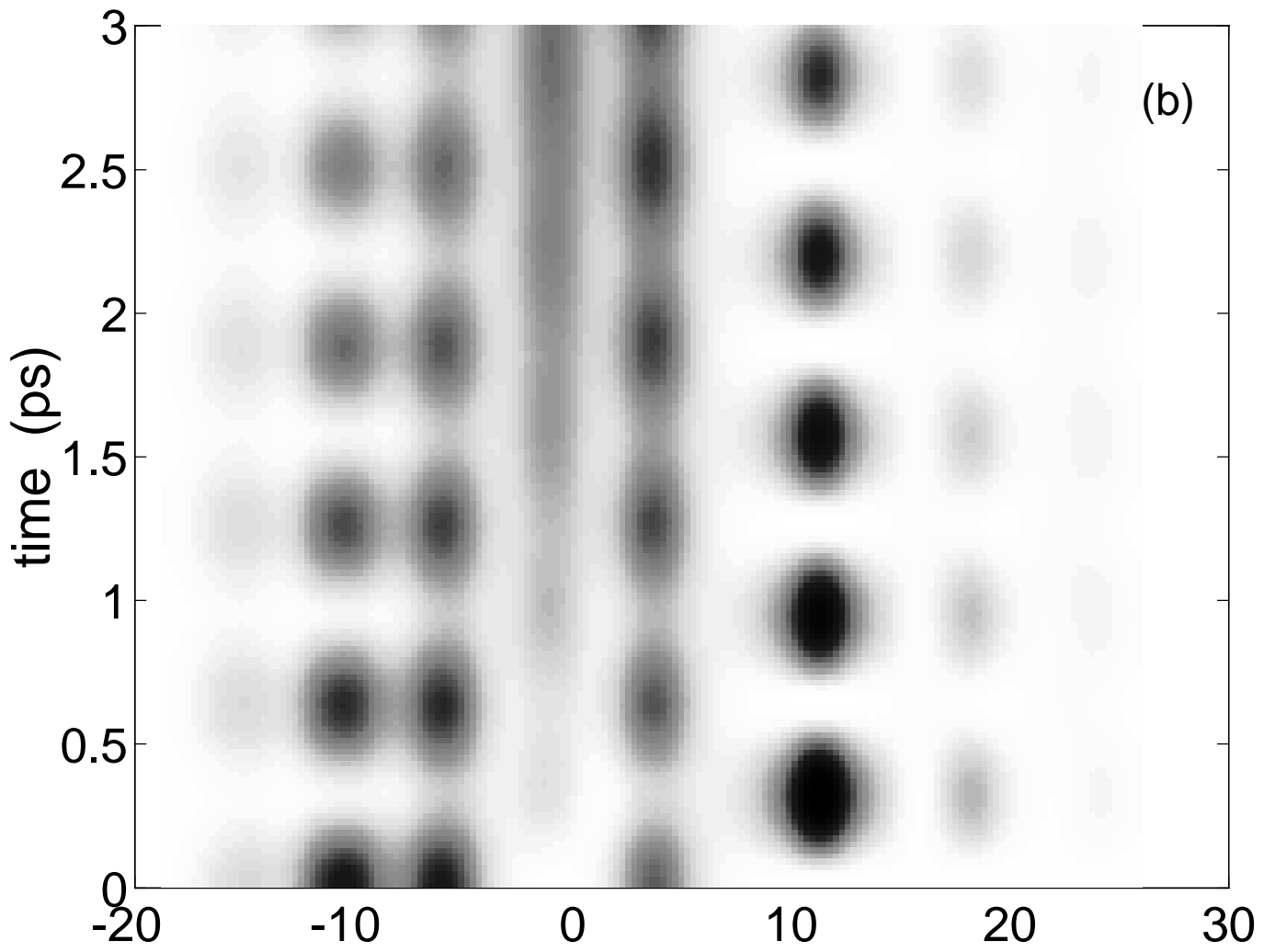
R. C. Iotti and F. Rossi, Figure 2(b)



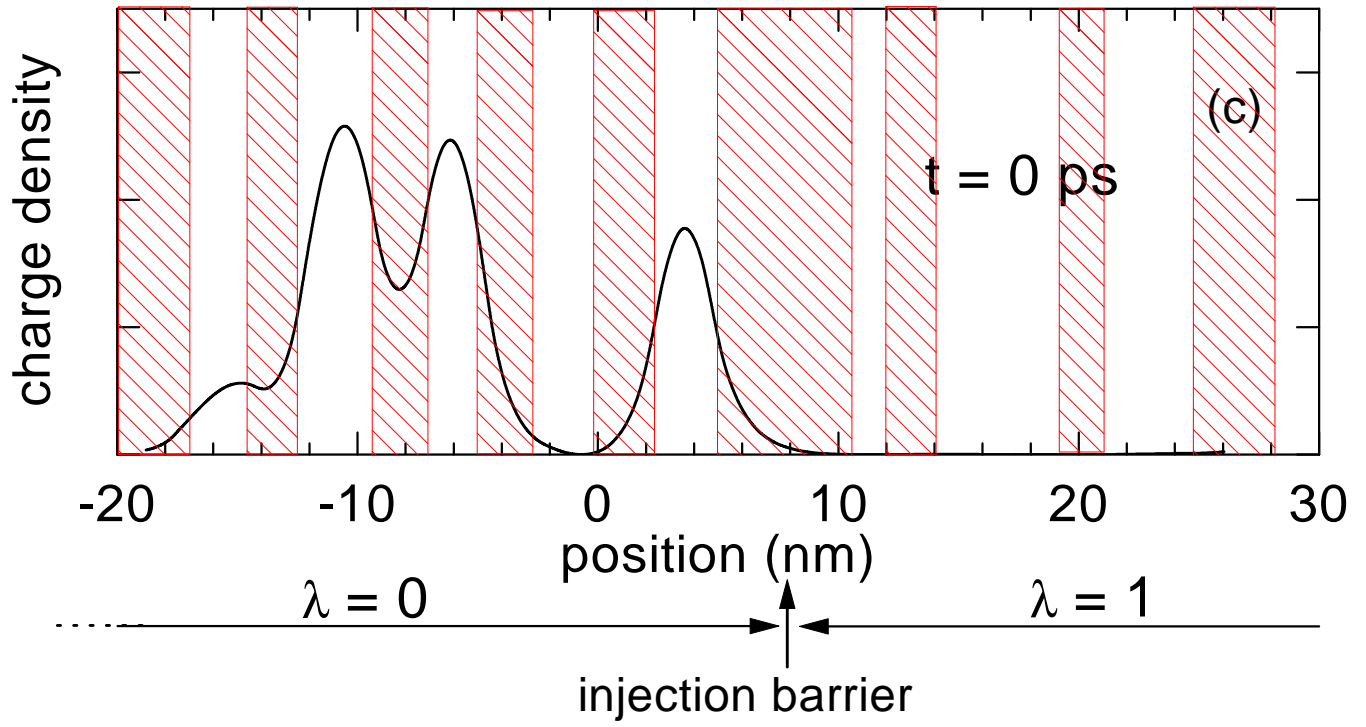
R. C. Iotti and F. Rossi, Figure 2(c)



R. C. Iotti and F. Rossi, Figure 3(a)



R. C. Iotti and F. Rossi, Figure 3(b)



R. C. Iotti and F. Rossi, Figure 3(c)